Argonne National Laboratory

A STUDY OF TRANSIENT HEAT TRANSFER FROM A WATER-IMMERSED ALUMINUM FUEL-PLATE SAMPLE IN TREAT

by

Lawrence J. Harrison

The facilities of Argonne National Laboratory are owned by the United States Government. Under the terms of a contract (W-31-109-Eng-38) between the U. S. Atomic Energy Commission, Argonne Universities Association and The University of Chicago, the University employs the staff and operates the Laboratory in accordance with policies and programs formulated, approved and reviewed by the Association.

TABLE OF CONTENTS

4

LIST OF FIGURES

LIST OF TABLES

A STUDY OF TRANSIENT HEAT TRANSFER
FROM A WATER-IMMERSED ALUMINUM
FUEL-PLATE SAMPLE IN TREAT

by

Lawrence J. Harrison

ABSTRACT

During a photographic study of the chemical reaction between water and aluminum-alloy plate-type fuel samples subjected to nuclear transients, time-elapse and energy-input data were obtained for incipient nucleate boiling, stable film boiling, and high-temperature physical and chemical responses of the sample. In this study, these data are used to calculate the transient temperatures, heat fluxes, and heat losses from the samples.

The modes of transient heat transfer considered are conduction, nucleate boiling, film boiling, and radiation, all under highly subcooled pool conditions. Calculations are begun at ambient temperature and are taken on past sample melting to high temperatures at which the chemical reaction occurs at a significant rate; one typical experiment had a calculated peak sample temperature of 1590°C. The transient energy-release rates were in the range from 100 to 200 msec, and all the experiments were conducted at 12.3 psia.

The temperature range considered in this study far exceeds the ranges previously reported in the literature, and this is the only study using reactor fuel as the heat source. This study includes plots of time versus reactor power, energy release, sample temperature, and events in the fuel during a typical transient.

I. INTRODUCTION

An important area of nuclear-reactor safety is heat transfer from the fuel during a nuclear transient. Experimental studies in this area are limited, undoubtedly because of the difficulty in simulating exponential energy releases and obtaining the necessary and desired data. Studies that were made under subcooled, stagnant-pool conditions have failed to produce predictive correlations, and only a very limited amount of empirical data

is available for application to critical facilities and low-power pool reactors that use plate-type fuel assemblies. A number of reactors also fall into this heat-transfer category when they are shut down for fuel charges.

The study of transient, subcooled, stagnant-pool heat transfer reported here is an outgrowth of a photographic study of plate-type fuel samples undergoing aluminum-water chemical reaction in TREAT.[1] In this study, high-speed motion pictures were obtained while a sample was being subjected to a nuclear transient. These pictures permitted the determination of various temperature-dependent responses, nucleate boiling, film boiling, sample melting, etc., as a function of sample energy input and time. These data are used to calculate the sample temperatures, heat fluxes, and energy-loss values at the times the various temperature-dependent events occurred. The study covers sample temperatures from room temperature to 2000°C.

All the experiments were performed at 12.3 psia, the normal atmospheric pressure at the TREAT reactor location. At this pressure, the boiling point of water is 95°C.

Rosenthal and Miller[2] appear to be the first to have studied transient, subcooled, stagnant-pool heat transfer up to burnout. Platinum and aluminum ribbons were electrically heated at exponential rates controlled by 100 thyratron tubes discharging in series. Ribbon-temperature and heat-flux data were listed for exponential periods ranging from 5 to 75 msec and for subcooling ranging from near 0 to 68°C. An extrapolation of their data obtained in a 33°C pool to the conditions of the study reported here gives a burnout heat flux of somewhat less than 75 cal/sec-cm^2 (1.0 x 10^6 Btu/hr-ft^2). Their study also indicates that for the conditions of the present study, nucleate boiling would begin when the sample reached saturation temperature.

Johnson et al.[3] conducted an extensive study over the same basic range of experimental conditions as Rosenthal and Miller using the same basic experimental equipment. No general correlation could be formulated to cover the Johnson data; the data are reported, however. Their conclusions include the following statements, which are directly relevant to the present study:

1. "The (nucleate-boiling-incidence temperature) overshoot behavior is severe when the subcooling of the liquid is great."

2. "The thermal capacity of the ribbon is found to be of great importance in its effect upon ribbon temperature, and (for thin ribbons) in its effect upon the burnout heat flux."

Only two of Johnson's experiments are comparable to the present study. In these two experiments, thin platinum ribbons were heated at

periods of 85 and 87 msec. The respective temperatures and heat fluxes at incipient nucleate boiling were 118 and 126°C, and 13 and 11 cal/sec-cm^2 (1.72 x 10^5 and 1.5 x 10^5 Btu/hr-ft^2). The respective burnout temperatures and heat fluxes were 206 and 198°C, and 117 and 136 cal/sec-cm^2 (1.55 x 10^6 and 1.80 x 10^6 Btu/hr-ft^2). The ribbons were in a horizontal attitude.

Lurie and Johnson[4] studied transient, subcooled, pool boiling on a vertical metallic ribbon subjected to one-step heating. In general, the results are not directly applicable, but one of their conclusions is relevant:

"In the subcooled case the liquid adjacent to the ribbon is highly superheated before nucleation of bubbles begins."

Miller[5] reported some transient, subcooled, pool heat-transfer data obtained in SPERT-I using full-sized fuel plates identical in construction to the alloy-plate samples used in the present study. The exponential periods ranged from 7 to 50 msec, and the pool apparently was at room temperature. For a 9-msec-period transient, the calculated heat flux at incipient nucleate boiling was 38 cal/sec-cm^2 (5 x 10^5 Btu/hr-ft^2). At the onset of film boiling, or at departure from nucleate boiling (DNB), the reported heat flux was 530 cal/sec-cm^2 (7 x 10^6 Btu/hr-ft^2). The temperature at DNB was measured as approximately 180°C. Miller did not observe a drop in sample temperature immediately following the onset of nucleate boiling; the temperature continued to rise, but at a linear rather than exponential rate. Johnson, as well as Rosenthal and Miller, reported a significant drop in ribbon temperature immediately following the onset of nucleate boiling. Miller attributes the nondropping of the sample temperature at the onset of nucleate boiling to the greater heat capacity of the SPERT-I fuel plates.

In a summary of a series of experiments covering pressures from ambient to 1000 psia, water-flow velocities from 0 to 14 fps, exponential periods from 5 to 50 msec, and subcooling from 0 to 62°C, Schrock et al.[6] state:

"The complexity of the problem is so great, however, that very detailed and accurate predictions are not yet possible for all aspects of the problem, particularly the void."

Hamill and Baumeister[7] have reported a theoretical analysis of subcooled film boiling and radiation heat transfer from flat plates. This analysis resulted in a steady-state correlation for determining total heat flux. No experimental data were presented for evaluation of the correlation.

II. EXPERIMENTAL TECHNIQUE

A. Summary

Briefly, the experimental technique entails placing a fuel-plate sample, approximately 3.5 by 1.3 cm, in a small pool of demineralized water at room temperature and pressure. The pool and sample are encapsulated and placed in the core of the TREAT reactor. A reactor transient is then run, resulting in a transient nuclear-energy release in the fuel sample. A high-speed camera outside the reactor records the thermally induced physical events, nucleate boiling, film boiling, sample melting, etc., which occur at the sample. The camera views the sample through windows in the capsule, a slot through the reactor core and reflector, and a series of mirrors to provide a line of sight through the reactor shielding. The events, which are recorded on film, are correlated with time and sample nuclear-energy release. These basic data are then used for the calculations reported here.

B. Reactor Description and Operation

TREAT is a thermal, graphite-moderated and -reflected, pulsed test reactor designed to meet the needs of various experimental reactor safety programs. Its engineering design is described elsewhere;[8] Fig. 1 presents a perspective of the reactor.
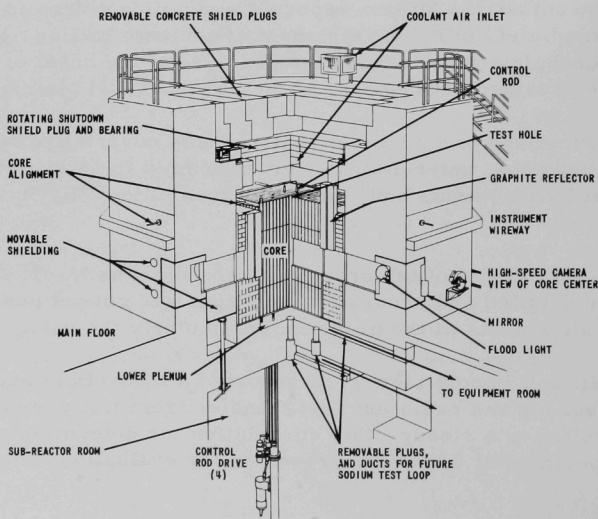
112-771

Fig. 1. TREAT Perspective

To permit the inserting and photographing of transparent capsule experiments in the reactor, slotted fuel assemblies have been fabricated. The central 2 ft of these assemblies do not contain any material except thin support members on two sides. Each assembly thus has an 8.25- by 56-cm opening. Placing a series of these assemblies in a row forms a slot of the above cross section from the center of the reactor to the reflector. A continuation of this slot has been built into the reflector and shielding, terminating at a movable shielding block to which a series of mirrors has been fastened. The camera, located outside the reactor shielding, views the experimental sample through the mirrors and slot, a total distance of approximately 4 m. The details of this in-pile photographic facility are described elsewhere.[9]

The following briefly describes the transient operation of the reactor for the experiments described here. The transparent autoclave is assembled (see Section C below for details) and inserted in the slot in the reactor core. For the reactor core loading used for these experiments, the sample is approximately 30 cm from the center of the core. The reactor is brought to a steady-state power level of 50 W, and the operation is then transferred to the automatic control system. This system turns on the capsule lights, starts the camera, starts the recording oscillograph, and releases the transient-initiating control rod; when a predetermined integrated reactor-power value is reached, the reactor is scrammed by the automatic control system. The oscillograph records the reactor power, integrated power, sample temperatures, timing lines, etc., and the camera records the physical responses of the sample. The camera runs until the entire reel of film is exposed, approximately 16 sec.

C. Description of Transparent Capsule

Figure 2 is a photograph of the disassembled transparent capsule used in these experiments. As can be seen, the capsule has three main parts: the water tube, the capsule, and the slot liner. Figure 3 is a photograph of the fuel sample in a water tube of the original design. The fuel sample is inserted into slots milled in the two graphite pins, which are inserted in the graphite block. This subassembly is lowered into the 0.16-cm-thick quartz-glass tube. The background was made by laying strips of black tape on the back of the tube and then covering the entire back with white RTV (room-temperature vulcanizing) silicone rubber. Approximately 100 cc of demineralized water is added to the water tube.

During the experiments, two modifications were made to the water-tube assembly. The first modification was required to eliminate darkening of the rectangular quartz-glass tubes during the transients. The tubes were originally extruded in a circular cross section and then drawn over a mandrel to obtain the rectangular shape. Apparently the tubes had absorbed impurities from the mandrel, resulting in radiation-sensitive tubes. These

tubes were replaced by U-shaped stainless steel tubes to which quartz-glass windows were attached with RTV silicone rubber. The striped background was made on a strip of thin stainless steel, which was inserted in the back of the water tube.

The second modification was the replacement of the solid graphite fuel-support pins with hollow alumina tubes. This modification reduced the heat loss from the sample to the support pins.

The capsule is designed to contain sample fragments, water, and glass fragments in the event of shattering of the water tube. The overall dimensions of the 16-gauge stainless steel capsule are 47 by 45 by 4.75 cm. The capsule window is made of high-purity glass, which is not discolored by radiation received in the reactor. This window is sealed inside a stainless steel frame with RTV silicone rubber. The frame is bolted to the capsule with a silicone-rubber gasket between the frame and the capsule. The small hook on the lower end of the window frame is used to withdraw the capsule from the slot liner following an experiment. To facilitate capsule purging, stainless steel tubing extends from the bottom of the capsule to the opening in the top of the capsule. Rubber tubing connects the top of the stainless tubing to the inlet line in the slot liner.
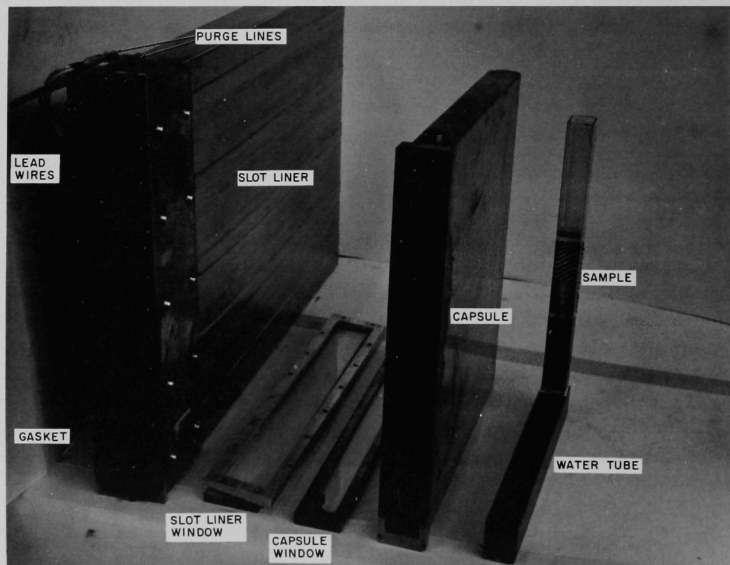
ID-103-7358 Rev. 1

Fig. 2. Disassembled Transparent Capsule

The 14-gauge, Type 304 stainless steel slot liner has overall dimensions of 53 by 86 by 7.6 cm. The high-purity glass window, which bolts on the front of the slot liner, mounts in a set of small dowels and is sealed by an exterior frame and a pair of silicone-rubber gaskets. The frame holds the window at a 5° angle to prevent the reflection of exterior light off this window into the camera. The front of the slot liner has been reinforced on both sides with stainless steel plates to restrict pressure-induced bowing of the sides, which could result in the gasket being blown out from behind the window and the loss of the leak-tight seal. An internal pressure of 32 psig will blow out the gasket, but at least twice that pressure can be contained if the sides of the slot liner are restrained by auxiliary supports, such as the fuel elements in the reactor. The back half of the slot liner is completely lined with reactor-grade graphite to act as a thermal barrier in the event fuel fragments melt through the capsule; in the assembled configuration, the capsule is thus enclosed on five sides by the graphite liner.

In the top of the slot liner near the window are lead wires, an electrical connector, and two purge lines. The electrical connector is potted in resin for a leak-tight seal. The inlet purge line is connected to the bottom of the capsule, and the outlet purge line begins at the bottom of the slot liner. A special handle bolts to the slot liner at the bottom of the window frame to facilitate inserting and withdrawing the assembly from the reactor. The slot liner is designed to provide leak-tight containment for fission gases released during the experiments and to provide backup containment for the capsule.

ID-103-7359

Fig. 3. Pretransient Fuel Sample Mounted in Water Tube

The lamps used to illuminate the samples are Sylvania 1000-W quartz-iodine "Sun-Gun" lamps. Each lamp is mounted in a stainless steel light shield with a built-in reflector. When these light units are mounted at the top and bottom of the capsule, the lamps are at a 30° angle with respect to the window to provide optimum photographic conditions.

After the three main parts of the capsule have been put together, the assembly is purged with helium to reduce the oxygen content to less than 2%, and the slot liner is leak-checked at 7 psig with a helium leak detector. After the internal pressure is reduced to atmospheric, the assembly is ready for insertion into the reactor.

D. Description of Samples

The individual fuel-plate samples are 1.5 cm wide and 3.5 cm high and are cut from a large plate, which was fabricated by the conventional "picture-frame" technique. This method of fabrication results in a sample whose heat-transfer surface is comparable to that in many reactors using plate-type, aluminum-clad fuel. The samples have a 0.051-cm-thick alloy fuel core; this uranium-aluminum alloy is 23 w/o fully enriched uranium. The fuel core is clad on both sides with 0.051-cm-thick Type 6061 aluminum. The alloy fuel samples are identical in composition and construction to the SPERT 1-D fuel.

E. Fission-energy Release

To determine the fission-energy release in the sample in the experiments, radiochemical analyses were made for the fission product molybdenum-99 in irradiated samples. A sample was placed in the autoclave as described in Section C above and subjected to a nuclear transient. The irradiated sample was then submitted to the Analytical Chemistry group of ANL-Idaho. Analytical results were obtained in the form of fissions per gram of sample; since the entire sample was dissolved for the analysis, the results were based on the total weight of fuel core and cladding. The fissions-per-gram value was then converted to a calibration factor of calories of fission energy released per gram of sample per megawatt-second of reactor power (cal/g-MWsec), assuming a prompt fission energy release of 172 MeV per fission. Only the prompt energy release is considered because a typical reactor transient, such as the one of experiment MWT-10, realizes 90% of the energy release in one-half second.

Of the 14 samples subjected to transient irradiation, the samples from experiments MWT-1, -2, and -8 were submitted for calibration analysis; in MWT-8 the sample was melted. Table I summarizes the results of these analyses.

TABLE I. Calibration Factors for Transparent Capsule
Experiments: Alloy-type Plate Samples

Experiment No.	Fissions/gram	Integrated Power, MWsec	Calibration Factor of Sample, cal/g-MWsec
MWT-1	1.58×10^{13}	31.5	3.30
MWT-2	3.20×10^{13}	65	3.24
MWT-8	8.00×10^{13}	157	3.35

Table I indicates that a calibration factor of 3.30 cal/g-MWsec can be used with a relatively high level of confidence. The results of MWT-8 indicate that sample melting and steam blanketing did not affect the neutron flux and resultant energy release in the sample.

F. Temperature Measurements

Posttransient examination of the first group of experiments in which the alumina support pins were substituted for the graphite pins (MWT-8, -9, -10, and -11) revealed that the sample tended to adhere to the alumina pins. Since the molten samples were thus maintaining a constant position for a significant period of time, it appeared possible to attach thermocouples to the samples and maintain contact, even though the samples were molten. To evaluate this possibility, Fiberglas-insulated, 0.025-cm-diam Chromel-Alumel thermocouples were installed in the samples for experiments MWT-13, -14, and -15. The technique developed entails drilling a 0.063-cm-diam hole, approximately 0.5 cm deep, into the edge of the sample. The thermocouple wires are twisted together and inserted in the hole, and the cladding on both sides of the hole is peened onto the junction. Normally, two thermocouples are used, one near the upper edge and the other near the lower edge of the sample. The lead wires are run down through the support pins, out the side of the graphite block, and on to an electrical connector, which mates with the connection potted into the slot liner.

The temperature data obtained from these three experiments appeared to be good. In MWT-13, and -15, the thermocouple wires were melted, indicating sample temperatures of at least 1430°C, the melting temperature of Chromel wire.

Bare 0.025-cm-diam tungsten/5% rhenium-tungsten/26% rhenium thermocouple wire was obtained to preclude thermocouple-wire melting. The junction was formed by welding the ends of the wires together with the lead-in sections covered by braided Fiberglas. These thermocouples were installed as described above, and good data were obtained in experiment MWT-18. The thermocouple signals were calibrated for a maximum signal above 1000°C, so that the thermocouple signals at the beginning of the transients were quite small and not accurate. There also appears to have been some thermal lag because of the extreme rise rates encountered. Other errors were induced by not knowing the exact location of the junction supplying the signal.

G. Photography Details

Before the first experiments were performed, trial photographs were taken. Various types of film, lamp configurations, camera settings, etc., were evaluated to determine the optimum conditions for the experiments. These trials resulted in the use of two quartz-iodine lamps operated

at 90 V each. Four-hundred-foot rolls of Ektachrome ERB high-speed color film were used in the Fastax WF-14 camera at a nominal film speed of 1000 frames per second. At this speed, 1 min of developed film projection shows approximately 1 sec of the experiment. A 15.25- or 25.4-cm lens was used, depending upon the field of view desired, at an f-stop setting of 4.5.

The camera has two separate lenses, which provide simultaneous photography of two separate view fields on each frame; one view is of the experiment fuel sample, and the other is of an oscilloscope screen. The oscilloscope shows a time signal with a short pulse every millisecond and a wide pulse every 10 msec. The oscilloscope also provides a reactor power signal with a pulse rate that is proportional to reactor power. Plotting the pulse rate as a function of time enables the point of peak power to be established on the film, and this point can be assigned the real-time value at which the peak reactor power occurred. The real time and the energy input at which each photographed event occurs are then readily obtainable. The technique is accurate to within 10 msec.

III. EXPERIMENTAL RESULTS

For the transient heat-transfer calculations, the significant results are the time and the integrated-nuclear-energy-release values at which the various temperature-dependent events initially occur. Table II summarizes the relevant experimental data. The unlisted experiments did not yield any data that could be used for the present study, and not all events could be seen in the films of the experiments listed in the table. Some of the scatter in the data is due to the relative position of an event in the transient power pulse. This is particularly true for those events that occur at the higher-energy releases. The data presented were obtained from a family of power pulses with various power peaks and transient widths. These factors obviously affect the time and energy-release values necessary to realize a particular event. The nucleate and film boiling were least affected by these variables in the experiments, since they both occur early in the transients.

TABLE II. Summary of Events: Alloy Fuel Samples

Exp No.	Period, sec	Nuclear Energy Release prior to Event, cal/g of Sample						
		Nucleate Boiling	Film Boiling	Sample Melt	Incandescence	Hydrogen Bubbles	Fine Al_2O_3	Fragmentation
MWT-4	0.139	-	-	270	391	None	None	None
MWT-9	0.113	-	-	224	298	322	None	None
MWT-10	0.108	-	-	307	361	-	411	None
MWT-11	0.108	26	-	231	297	330	537	726[a]
MWT-12	0.108	-	-	224	320	349	512	747
MWT-13	0.115	26	66	267	379	469	None	None
MWT-14	0.285	24	69	None	None	None	None	None
MWT-18	0.109	-	-	247	373	535	547	772
	Average:	25.3	67.5	253 +54 −29	346 +45 −49	401 +134 −79	502 +45 −91	748 +24 −22

[a]This fragmentation occurred after the transient (see Fig. C.4).

Nucleate boiling is defined in this study as the appearance of short-lived, discrete steam bubbles. Initially these bubbles have a diameter of about 0.06 cm. The reflection of light off the vapor-liquid interface reveals their presence.

Film boiling is defined in this study as the appearance of a stable vapor film over the vertical face of the sample. Again, the reflection of light off the undulating vapor-liquid interface reveals the presence of the film boiling. This is probably stable film boiling and occurs later in the transient than the point of DNB.

The relevant data are presented more completely in Appendix C, where each experiment is represented graphically and tabularly. The time scales used for these presentations have arbitrary zero values.

IV. METHOD OF CALCULATION

A. Introduction

The calculations reported here are divided into three segments, each covering different heat-transfer conditions. The first segment covers conduction heat transfer from the initiation of the transient until nucleate boiling begins; the second segment, nucleate and film boiling up to sample melting; the third segment, film boiling on the molten sample.

For the first two calculational segments, experiment MWT-13 is taken as a representative experiment. The energy-release rate and the time of occurrence for nucleate boiling, film boiling, and sample melting are those experimentally determined. The molten-sample calculations are based on the average energy-release values for any given event as presented in Table II.

B. Conduction Heat Transfer

Before nucleate boiling, the heat-transfer mechanism is assumed to be only conduction through the fuel sample and water. This assumption is based on the fact that the vertically oriented sample is immersed in a pool of stagnant water, and the time interval for significant energy release under these conditions is less than 0.6 sec. The literature contains several references[2-4,6] to the same assumption for similar conditions. In support of this assumption, the calculated thermal-expansion rate of the 0.025-cm-thick layer of water adjacent to the sample is 10 cm/sec at the time nucleate boiling begins, at the same time the expansion rate for the upper edge of the fuel sample is 17 cm/sec, thus counteracting the initial natural convection effect.

The THTB[10] computer program is used for the first calculational segment, i.e., the conduction heat transfer. The program is highly flexible and for this study incorporates a variable internal-heat-generation rate, temperature-dependent physical properties, a time-increment value of 0.01 sec, and unidirectional heat flow. The program uses the general heat-balance equation for each calculational node to calculate the node central temperature, using the input data provided. The process is repeated for each time increment.

The calculational model is a 0.025-cm-square segment of one-half of the fuel sample, i.e., one-half of the fuel core, the cladding on one side, and the adjacent water. The 0.025-cm-thick fuel is the first node, followed by two 0.025-cm-thick nodes of cladding. At the surface of the model fuel sample are three nodes of 0.025-cm-thick water, followed by a 0.025-cm-thick bulk-water heat sink with a high heat capacity.

At time zero in a reactor transient, the reactor is operating at a power level of 50 W, which results in a sample energy-release rate of 1.65×10^{-4} cal/g-sec. The reactor power rises to approximately 1 MW in 1.0 sec, and at this time the computer calculation is begun, since the energy-release rate in the sample has reached a significant level. During the initial 1.0 sec, approximately 0.5 cal/g of sample has been released, but this value is not considered. The conduction calculation is terminated 0.57 sec later, the time of incipient nucleate boiling, thus giving the heat-transfer conditions immediately before nucleate boiling.

C. Boiling Heat Transfer up to Sample Melting

The lack of transient, subcooled, pool-boiling correlations and data increases the difficulty of calculating the heat transfer from the sample. To circumvent this problem, the physical properties of the sample, the energy-release data, and the time-of-event data for initial nucleate boiling, film boiling, and sample melting are used to calculate heat-transfer conditions at specific times. Starting at sample melting, the calculations are carried back to the time the sample initially attains the melting temperature, to the time of initial film boiling, and to the time of initial nucleate boiling; i.e., the calculations are performed in reverse of the actual sequence of events. Thus the end of this calculation coincides with the end of the conduction calculation.

The calculation begins at the time the sample melts, because the sample heat content (assuming no solid-state superheating of the sample), the sample energy release, and the sample temperature are known at this time. To determine the time the sample initially attains the melting temperature, the following are subtracted from the sample energy release at the time the sample melts: (a) the heat of fusion of the sample, and (b) the heat loss from the sample while the heat of fusion is being released in the sample. The result is the energy release in the sample when the melting temperature is attained, and the corresponding time value is directly determined from the energy-release-versus-time data. While the heat of fusion is being released, the sample is steam-blanketed and loses heat primarily by film boiling, together with a small amount of radiant heat transfer.

To calculate the heat-transfer conditions at the time of initial film boiling, a trial-and-error energy balance is made from the time the sample initially attains its melting temperature back to the time of initial film boiling. When the sample initially attains its melting temperature, the time, the sample energy release, and the sample temperature are known. At the time of initial film boiling, the time and the sample energy release are known. The two unknowns in the energy-balance equation are the film-boiling heat loss and the sample temperature at the time of initial film boiling; these two values are determined by the calculation. The time of initial film boiling is approximately equal to the time of maximum nucleate-boiling heat flux.

A stable film-boiling coefficient was calculated by use of Bromley's[11] correlation for saturated film boiling and was applied to the subcooled film-boiling condition of this calculation. The coefficient probably would be higher for subcooled boiling, but Bromley's data do not indicate a gross change in the coefficient value over a temperature differential change of a few hundred degrees centigrade. Since the same basic mechanism is involved, Bromley's data should be indicative of the order of magnitude of change involved in the subcooled case. Thus, the calculated coefficient should be satisfactory for this calculation.

The overall heat-transfer coefficient from the steam-blanketed sample fuel plate at 640°C, the sample melting temperature, was also calculated by using the theoretically derived correlation of Hamill and Baumeister.[7] In this instance, there is no significant difference between the Hamill and Baumeister coefficient and the Bromley coefficient. Appendix B contains sample calculations of the two coefficients.

The following assumptions are made to facilitate the calculation of heat-transfer conditions during the transient nucleate boiling:

1. The temperature gradient across the sample is directly proportional to the surface heat flux.

2. The sample temperature at initial nucleate boiling is equal to the sample temperature determined by the final conduction calculation.

3. The mean sample temperature at the peak nucleate boiling is equal to the mean sample temperature calculated for initial film boiling.

4. The mean nucleate-boiling heat flux occurs at a mean sample temperature equal to the mean between the final sample temperature determined by the conduction calculation and the sample temperature at initial film boiling.

5. The nucleate-boiling heat flux is proportional to the energy-release rate in the sample and the cube of the difference between the bulk water temperature and the sample surface temperature.

These assumptions, together with the calculated mean heat flux, permit the initial and final nucleate-boiling heat-flux values and the sample surface temperature at the peak flux to be calculated.

D. Heat Transfer from a Molten Sample

The temperature range beyond the melting point of the fuel sample is important, because it is in this range that the rate of chemical reaction between aluminum and water becomes significant. Such a calculation cannot be precise because of many imprecisely known values, such as the energy input at the time of an event, surface area, and surface emissivity. The following assessment can be made, however.

Table II lists the average energy release at the time of any given event in this series of experiments. The average energy release required to take a sample from melting to vapor-phase chemical reaction is 261 cal/g. Using this energy value, together with a sample heat capacity of 0.24 cal/g-°C and the 640°C melting temperature, one can calculate a sample temperature of 1730°C for the beginning of the vapor-phase chemical reaction. It has been established[1] that the vapor-phase chemical reaction has a threshold temperature of 1750°C. Based on this calculation, it appears that the heat loss and energy release from the molten sample are within the overall accuracy range of the values for sample heat capacity, energy release at the time of event, etc., for the molten sample.

The same technique can be used to calculate an approximate sample temperature for those events that occur within the range of 640 to 1750°C. This technique is not satisfactory for calculating the sample fragmentation, however.

V. RESULTS AND DISCUSSIONS

A. Conduction Heat Transfer

The THTB program calculated the temperature of each of the seven nodes in the model on 0.01-sec intervals up to the time of incipient nucleate boiling, a period of 0.57 sec. Figure 4 presents the temperature profile across the calculational model at the time of incipient nucleate boiling. As can be seen from the figure, the cladding surface temperature is 126°C at this time, and the mean sample temperature is 127°C.
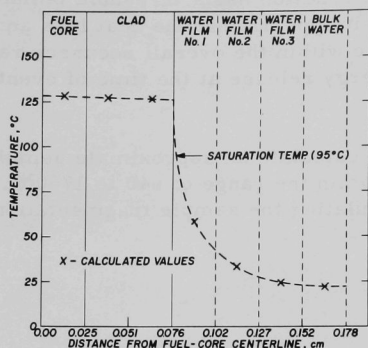
ID-103-7585

Fig. 4. Calculated Temperature Profile at Incipient Nucleate Boiling: Experiment MWT-13

The temperature profile drawn between the calculated points indicates a superheated water layer, approximately 0.002 cm thick, adjacent to the sample. The exact thickness and temperature of a superheated layer are open to discussion, but the profile presented should give some indication of the true situation.

The calculated conduction heat flux at the time of incipient nucleate boiling is 6 cal/sec-cm^2. The heat loss from the sample during conduction is calculated from the temperature increase of the water and has a value of 4.5 cal. Sample and water temperatures as a function of time are presented later in Fig. 5, together with data that cover sample temperature up to film boiling.

B. Boiling Heat Transfer up to Sample Melting

From physical property data,[12] the sample energy content at melting is known to be 248.5 cal/g with a heat of fusion of 80 cal/g. In the high-speed films, the sample is seen to melt at 1.89 sec, and it has been calculated that the heat of fusion is released in the sample during the preceding 0.06 sec. From Bromley's film-boiling correlation, the heat flux from the 640°C sample during the 0.06-sec interval is 3.3 cal/sec-cm^2. The total heat loss during this interval is approximately 1 cal/g and does not change the time interval during which the sample is at 640°C. Bromley's correlation yields a radiation loss of 3.5% of the total loss, the total loss being slightly over 1% of energy released while the sample is at 640°C.

To determine the sample temperature at the time film boiling begins (1.69 sec, as seen in the high-speed films), a series of energy-balance calculations is made from 1.83 sec back to 1.69 sec; the energy

release, the sample heat content, and the heat loss are included in the calculations. This calculation results in a mean sample temperature of 227°C at initial film boiling. The mean film-boiling heat flux from 1.69 to 1.83 sec, based on a mean sample temperature of 433°C, is 2.2 cal/sec-cm^2. The energy release during this interval is 120 cal/g, and the heat loss is approximately 1.5 cal/g, with the radiation loss being insignificant.

For the time periods and sample temperatures realized during film boiling, any chemical reaction that occurred between the aluminum and water did not release sufficient energy to be significant, based on the experimental study of the chemical reaction.[1]

During the 0.12 sec of nucleate boiling, the mean sample tempera-ture increases from 127 to 227°C, the sample heat content increases from 26 to 50 cal/g, and the energy release is 40 cal/g; the heat loss thus equals 40% of the energy release. Using this value together with the energy release data and the assumptions listed in Section IV.C, the calculated incipient-nucleate-boiling heat flux is 5 cal/sec-cm^2 and the peak-nucleate-boiling heat flux is 88 cal/sec-cm^2. The value of 5 cal/sec-cm^2 is in reasonable agreement with the value of 6 cal/sec-cm^2 determined by the transient conduction calculation, considering the assumptions incorporated in the transient-nucleate-boiling calculation.

Based on the preceding conduction and film-boiling heat-transfer calculations and the assumptions listed in Section IV.C, the mean sample temperature and the sample surface temperature at incipient- and peak-nucleate-boiling heat flux are as follows: At incipient nucleate boiling, the sample surface temperature is 126°C and the mean sample tempera-ture is 127°C. At peak-nucleate-boiling heat flux, the sample surface temperature is 213°C and the mean sample temperature is 227°C.

Table III summarizes the transient heat-transfer conditions in experiment MWT-13 as determined by the conduction and film-boiling calculations and the assumptions in Section IV.C. This table is based on a calculational model 3.81 cm high by 0.13 cm wide by 0.076 cm thick with unidirectional heat flow.

TABLE III. Calculated Transient Heat Transfer through Sample Melting

Heat-transfer Condition	Time Interval, sec	Final Sample Heat Content, cal	Final Surface Temp, °C	Integrated Energy Release, cal	Calculated Time-interval Heat Loss, cal
No transfer	0 → 1.00	4	22	0	0
Conduction	1.00 → 1.57	27	126	27	4.5
Nucleate boiling	1.57 → 1.69	51.5	213	68	16.5
Film boiling	1.69 → 1.83	173	640	191	1.5
Film boiling at 640°C	1.83 → 1.89	256	640	275	1

Figure 5 presents the calculated sample temperatures up to the time of initial film boiling and the water-film temperatures up to the time of initial nucleate boiling. Also presented are the temperatures indicated by the two thermocouples located in the sample. These thermocouples were calibrated for a full-scale reading of 1500°C; thus their signals in the range under consideration are not very accurate. The shape of the thermocouple values as a function of time are in general agreement with the shape of the calculated values, with some thermal lag apparent. The thermocouples do indicate, however, a much lower sample temperature at the time of initial film boiling, which would be indicative of higher heat-flux values during nucleate boiling. The overall accuracies of the calculated and indicated values are such that the disagreement may not be significant.

ID-103-7587

Fig. 5. Calculated and Indicated Sample Temperatures up to Film Boiling: Experiment MWT-13

Table IV presents the only data found in the literature which are comparable to that reported immediately above. Also presented are the sample surface temperatures at incipient nucleate boiling (N.B.) and initial film boiling (F.B.) and the heat-flux values at incipient and maximum nucleate boiling.

TABLE IV. Comparison of Surface Temperature and Heat Flux at Boiling Conditions

Reference	$T_{N.B.}$, °C	Q/A for Nucleate Boiling, cal/sec-cm^2 Incipient	Maximum	$T_{F.B.}$, °C	Period, msec
This study	126	5	88	213	100-200
Rosenthal & Miller[a]	100	NA	<75	NA	~100
Johnson et al.[b]	118	13	102	121	85
Johnson et al.[b]	117	11	106	157	87

[a]Extrapolated, ambient pool temperature.
[b]Horizontal ribbon, pool water temperature = 37.5°C.

In all the referenced experimental data, a small thin platinum ribbon was electrically heated. When incipient nucleate boiling was attained, the ribbon temperature fell because of the rapid heat dissipation from the low-thermal-capacity ribbon. Miller[5] reports no drop in the sample temperature, as evidenced by no brief disappearance in the steam bubbles at initial nucleate boiling, contrary to the results reported by the

two reference studies in Table V. Miller attributes nondropping of the sample temperature to the finite heat capacity of his sample. In the present study, there was no evidence of a drop in sample temperature, i.e., no temporary disappearance of steam bubbles at the time of initial nucleate boiling. This apparently is due again to the finite heat capacity of the sample.

The various comparative values presented in Table IV do not agree precisely. This is not unexpected, since the experimental conditions and techniques and the calculation methods are different. Rationalizing the various differences is virtually impossible, but the following evaluation can be made.

In this study, a small error in determining the time of initial film boiling seen in the films would significantly change the results because of the high energy-release rate in the sample at the time. The initial film-boiling temperature could thus be lower, and the maximum nucleate-boiling heat-flux value could be greater. Since only stable film boiling could be seen in the films, the sample temperature reported here for initial film boiling is higher than would be reported if point of departure from nucleate boiling (DNB) could have been determined. In the reference works, DNB is reported; thus it is not surprising that high sample temperatures and low heat-flux values were determined. In addition, Johnson[3] states that the thermal capacity of the heating surface is of great importance in its effects upon the burnout heat flux. Further elaboration on this point is lacking.

The data reported here cannot be taken as precise, because there are obvious sources of error. For example, (a) the time of occurrence for a given event has an accuracy range of ± 0.01 sec, because the initial event had to be picked off moving film rather than from individual frames; (b) the energy-release data obtained from the reactor is at the low end of the data scale thus possessing an inherently larger accuracy range; and (c) a small change in energy-release or heat-content values can result in a significant change in sample temperature.

These errors could not be avoided, since the experiments were not designed as heat-transfer experiments and the heat-transfer calculation had to be made with the information that was available. The data do, however, give a good indication of the events and their corresponding values in an area that has not been empirically considered before. Many of the test conditions are typical of a number of reactors; the fuel-sample construction is typical of many reactor fuels, the surface condition of the sample is typical of plate-type aluminum fuel, and the water quality is typical of the water quality in many reactors. The applicability of the energy-release period depends, however, on the system being considered.

C. Heat Transfer from a Molten Sample

This study has been continued beyond the melting points of the alloy fuel sample. This upper temperature range is highly significant, because here the rate of chemical reaction between aluminum and water becomes significant during reactor transients. Calculations in this range cannot be precise, because of the many unknowns, such as surface emissivity and surface area. The following evaluations can be made, however.

Table II shows that the average energy release from sample melting (640°C) to the formation of fine Al_2O_3 reaction product ($1750°C^1$) is 270 cal/g. With a sample heat capacity of 0.24 cal/g-°C* for the range, the energy required to effect this temperature change is 274 cal/g. This shows that the heat loss between sample melting and the formation of fine Al_2O_3 (0.18 sec in MWT-11) and the energy released from chemical reaction during the same interval are within the range of the overall accuracy. The heat loss from the sample is expected to be small, since the time interval is short, and the sample is roughly spherical in shape, is steam blanketed, and has a low emissivity. A small chemical-energy release is to be expected, since the time interval is short, and during most of this interval the chemical reaction rate is low because of the relatively low sample temperature.

The average energy release between sample melting and sample incandescence (0.05 sec in MWT-11) is 90 cal/g. This energy release, assuming no loss and a sample heat capacity of 0.24 cal/g-°C, will increase the sample temperature approximately 375°C. Thus, the sample temperature at the time of initial incandescence, as seen in the films of the experiments, is approximately 1000°C. This temperature is somewhat higher than would be anticipated, but the camera speed, the lens setting, the distance between the camera and the sample, the water, the windows, and the film development all can increase the temperature required to photograph incandescence.

With the above calculational method, the sample temperature at the time discrete hydrogen bubbles are seen is 1250°C. Thus, the various physical events seen in the films can be used as indications of sample temperature. Table V summarizes these physical events and their corresponding temperatures.

TABLE V. Physical Events as a Function of Sample Temperature in MWT Experiments

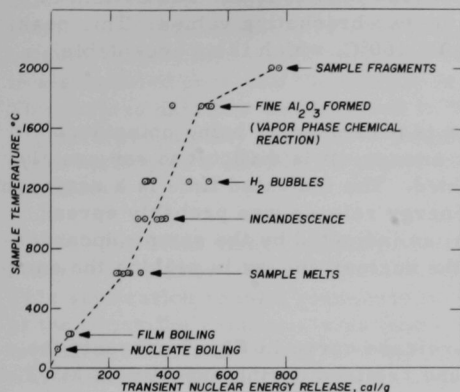| Physical Event	Sample Temperature, °C	Surface Temperature, °C	Physical Event	Sample Temperature, °C	Surface Temperature, °C
Nucleate boiling	127[a]	126[a]	Hydrogen Bubbles	1250[a]	
Film boiling	227[a]	213[a]	Fine Al_2O_3 formed	1750[c]	
Sample melting	640[b]		Sample fragmentation	2000[c]	
Incandescence	1000[a]				

[a]Calculated here.
[b]Ref. 17.
[c]Experimentally determined.[1]

*Refer to Appendix A.

Tables II and V can be used to plot sample temperature against transient nuclear-energy release; this plot is presented in Fig. 6. As can be seen in this figure and Table II, there is a significant scatter in the energy input for most temperature values, i.e., for most physical events. Part of the scatter is due to the relative position of a given energy-release value in a transient. For example, if an event occurs well past the peak power of a transient, the energy input at the time of event will be greater than it would be for the same event occurring before peak power. Also, at the higher temperatures, the molten samples are being distorted by internal gas pressure,[1] which undoubtedly affects the physical events that occur at the surface of a sample. Other errors contributing to the scatter have been discussed in other parts of this report.
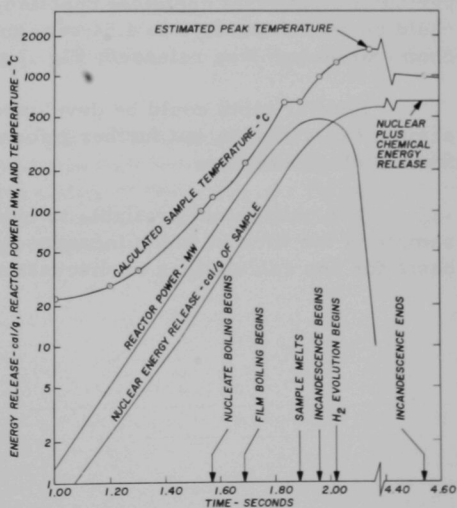

ID-103-7606

Fig. 6. Alloy Fuel Sample Temperature vs Nuclear-energy Release: MWT Experiments

In spite of the scatter, Fig. 6 does provide a means for estimating the temperature attained in transients similar to those of the MWT series of experiments. The line drawn in the figure passes through the average energy-release value for the various events.

Applying the temperature-event data of Table V to MWT-13 beyond the sample-melting event, together with the calculated sample temperature history before melting, enables sample temperature to be plotted against time, as shown in Fig. 7. Figure 7 also shows reactor power and sample energy release plotted against time. This figure thus presents a unique time, temperature, energy-release, and event history for an alloy fuel sample subjected to a nuclear transient.

The estimated peak sample temperature presented in Fig. 7 (1590°C) was determined as follows: The sample was

ID-103-7607

Fig. 7. Reactor Power, Sample Nuclear-energy Release, and Calculated Sample Temperature: Experiment MWT-13

instrumented with Chromel-Alumel thermocouples, which melted, thus showing a peak sample temperature of at least 1430°C. The films of the experiment did not indicate any vapor-phase chemical reaction, thus showing a peak sample temperature of less than 1750°C. The estimated peak value of 1590°C is the mean of the two bracketing values. This peak value could also be presented as 1590 ± 160°C, which is an acceptable range.

The time of peak temperature is presented as being coincident with the complete release of nuclear energy. It is difficult to say exactly when the peak temperature was attained. The indicated time is a reasonable approximation, since the chemical-energy release was probably spread over a relatively long period of time, as indicated by the sample incandes- cence, thus being less effective than the nuclear energy in peaking the sample temperature.

The upper end of the energy-release curve in Fig. 7 presents the nuclear- plus chemical-energy release realized during experiment MWT-13. The release rate of the chemical energy is not known, primarily because of the unknown surface area during this time.* Based on the appearance of discrete, reaction-product hydrogen bubbles, however, the sample tempera- ture must be in the 1250°C range to achieve a significant reaction rate. By going back to the incandescence temperature of 1000°C, one obtains an approximation of the time interval during which most of the chemical energy is released; i.e., the period of incandescence is approximately equal to the period of significant chemical reaction rate. In MWT-13, incandescence could be seen from 1.96 to 4.54 sec, and during this period the 80 cal of chemical energy was released; Fig. 7 presents these values.

Similar plots could be developed for the remaining MWT alloy- sample experiments, but further information would probably not be obtained from such an exercise.

The only datum available to indicate the cooling rate of a molten sample is the time at which incandescence ends. This datum is insufficient basis for any calculations or discussion.

---

*Reference 1 discusses sample distortion in the temperature range being considered.

VI. CONCLUSIONS

By the use of different calculation methods, it has been possible to calculate sample temperatures, heat fluxes, and heat losses from a small aluminum-clad fuel-plate sample subjected to a nuclear transient. The calculations include conduction, nucleate boiling, film boiling, and radiation in a subcooled pool with the sample in both the solid and molten states. The various data are summarized in Tables III and V and in Figs. 4-6. Figure 6 graphically presents a unique energy-release, temperature, and event history of a sample subjected to a relatively high-energy nuclear transient.

The most direct application of these data is to the experimental study of aluminum-water chemical reactions during a nuclear transient.[1] This application results primarily in determination of sample temperatures at the times the various events (nucleate boiling, film boiling, sample incandescence, and hydrogen bubble formation) were seen in the high-speed films taken during the transient experiments. This application also results in determination of the approximate time intervals during which the chemical reaction, as determined in Ref. 1, occurred in the various transient experiments.

The results of the present study can also be used in evaluating potential aluminum-water reactions during postulated nuclear transients in certain other reactors. The results are particularly applicable since the fuel-plate samples studied were fabricated identically to production fuel for reactors using plate-type, aluminum-clad fuel assemblies. Also, the water quality in the experiments is nearly identical to the water quality in some pool-type reactors.

The results of this study are unique in transient, subcooled, pool heat transfer since the range of conditions covered has not previously been reported in the literature. The applicability of these results to any problem will have to be evaluated on the basis of the comparability of this study to the problem under consideration.

APPENDIX A

Heat Capacity and Enthalpy of Alloy Fuel

The heat capacity of aluminum and uranium below 640°C is contained in many locations in the literature. The heat capacity of the core alloy of the fuel plates used in this study was calculated on an additive basis; i.e., the core alloy is 23 w/o uranium and 77 w/o aluminum, and the same percentage values are applied to the elemental heat capacities and summed to obtain the alloy heat capacity. The same method was used for the sample heat capacity. Table VI lists the results of the calculation.

TABLE VI. Heat Capacity of Aluminum, Uranium,
Core Alloy, and Total Sample

| Material | Heat Capacity, cal/g-°C | | | |
	0°C	200°C	400°C	600°C
Aluminum	0.208	0.235	0.258	0.282
Uranium	0.0275	0.0393	0.0368	0.0452
Core alloy	0.166	0.188	0.207	0.227
Total sample	0.196	0.218	0.236	0.259
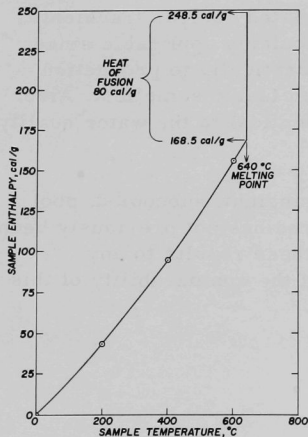
ID-103-7586

Fig. A.1. Enthalpy of Alloy Fuel Sample

These values are put into the THTB computer program, which linearly interpolates between the given points.

Based on the above values and the heat of fusion of the sample, the sample enthalpy curve presented in Fig. A.1 is determined.

To determine the sample heat capacity beyond melting, the following method was used. The literature indicates that when aluminum melts, its heat capacity decreases approximately 10%.[13] The 600°C value of 0.259 cal/g-°C was thus reduced to 0.24, and, to partially accommodate the increasing chemical-energy-release rate as the sample temperature increased, this value is used for the molten sample independently of sample temperature. The error involved in the method is probably not greater than the error resulting from data scatter in this study.

APPENDIX B

Calculation of Film-boiling Coefficient

1. Bromley[11]

$$h = h_c + h_r = 0.62 \left[\frac{g\rho_v(\rho_1 - \rho_v) \, \lambda_{va} k_v^3}{D\mu(T_s - T_1)} \right]^{1/4} + \frac{\epsilon\sigma(T_s^4 - T_1^4)}{T_s - T_1},$$

where

h_c = convection coefficient, $Btu/hr\text{-}ft^2\text{-}°F$;

h_r = radiation coefficient, $Btu/hr\text{-}ft^2\text{-}°F$;

g = gravity acceleration = 4.17×10^8 ft/hr^2;

ρ_v = vapor density = 0.023 lb/ft^3;

ρ_1 = liquid density = 60.2 lb/ft^3;

λ_{va} = difference in heat content between mean-temperature vapor and saturated liquid = 1180 Btu/lb;

k_v = vapor thermal conductivity = 0.027 $Btu/hr\text{-}ft\text{-}°F$;

D = plate width = 0.125 ft;

μ = vapor viscosity = 5.1×10^{-2} $lb_f/ft\text{-}hr$;

T_s = heating-surface temperature = $1645°R$;

T_1 = liquid temperature = $532°R$;

ϵ = heating-surface emissivity = 0.10;

σ = Boltzmann's constant = 0.1714×10^{-8} $Btu/hr\text{-}ft^2\text{-}°R$;

and

$$h = 1.3 + 35.5 = 36.8 \; Btu/hr\text{-}ft^2\text{-}°F.$$

This sample calculation is for the steam-blanketed fuel sample at 640°C.

2. Hamill and Baumeister[7]

$$q_{tot} = h_{tot}(T_w - T_s),$$

where

q_{tot} = total heat flux, $Btu/hr\text{-}ft^2\text{-}°R$;

T_w = wall temperature, $°R$;

T_s = saturation temperature of liquid, $°R$;

$$h_{tot} = h_{fb} + 0.88 h_{rad} + 0.12 h_{tcl}\, \theta;$$

$$h_{fb} = 35.5 \text{ Btu/hr-ft}^2\text{-}°F \text{ (from Bromley}[11]);$$

$$h_{rad} = 13 \text{ Btu/hr-ft}^2\text{-}°F \text{ (from Bromley}[11]);$$

h_{tcl} = turbulent liquid free-convection coefficient, Btu/hr-ft^2-°F;

$$h_{tcl} = 0.14 \left[\frac{k_1^3 \rho_1^3 g B_1 (T_s - T_b)\, Pr_1}{\mu_1^2} \right]^{1/3};$$

(see Section 1 above for some term definitions)

Pr_1 = Prandtl number = 1.75;

h_{tcl} = 2.2 (horizontal, upward-facing plate);

θ = subcooling parameter $(T_s - T_b)/(T_w - T_s)$;

T_s = saturation temperature, °F;

T_b = bulk-liquid temperature, °F;

T_w = wall temperature, °F;

θ = 0.135;

and

$$h_{tot} = 36.6 \text{ Btu/hr-ft}^2\text{-}°F.$$

This calculation is for the steam-blanketed fuel sample at 640°C.

APPENDIX C

Summary of Experiments

TABLE VII. Tabular Summary of Experiment MWT-4

Summary of Reactor Data

Transient No.:	851
Integrated power:	159 MW-sec
Reactor period:	0.139 sec
Peak reactor power:	306 MW

Summary of Experimental Data

Fuel sample:	SPERT 1-D, 2.069 g
Sample nuclear-energy input:	524 cal/g of sample
Energy released, Al + H_2O reaction:	0 cal

Summary of Events

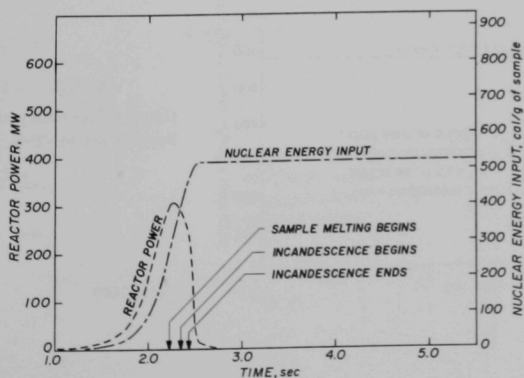|	Time, sec	Integrated Nuclear Energy, cal/g
Nucleate boiling begins	Not seen	NA
Film boiling begins	Not seen	NA
Sample melting begins	2.225	270
Incandescence begins	2.345	391
Hydrogen evolution begins	None	NA
Al_2O_3 evolution begins	None	NA
Fragmentation occurs	None	NA
Incandescence ends	2.435	NA

Fig. C.1

Graphical Summary of Experiment MWT-4

ID-103-7588

34

TABLE VIII. Tabular Summary of Experiment MWT-9

Summary of Reactor Data

Transient No.:	930
Integrated power:	177 MW-sec
Reactor period:	0.113 sec
Peak reactor power:	468 MW

Summary of Experimental Data

Fuel sample:	SPERT 1-D, 2.096 g
Sample nuclear-energy input:	584 cal/g of sample
Energy released, Al + H_2O reaction:	96 cal

Summary of Events

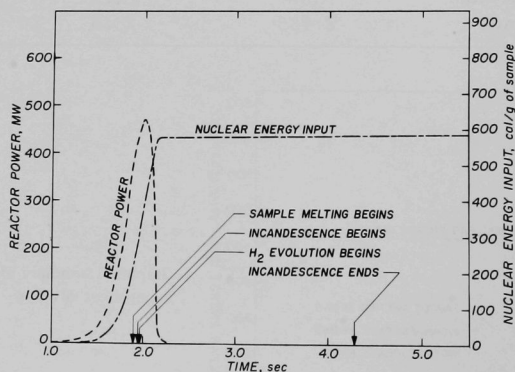|	Time, sec	Integrated Nuclear Energy, cal/g
Nucleate boiling begins	Not seen	NA
Film boiling begins	Not seen	NA
Sample melting begins	1.88	224
Incandescence begins	1.93	298
Hydrogen evolution begins	1.95	322
Al_2O_3 evolution begins	None	NA
Fragmentation occurs	None	NA
Incandescence ends	4.29	NA

Fig. C.2

Graphical Summary of Experiment MWT-9

ID-103-7589

TABLE IX. Tabular Summary of Experiment MWT-10

Summary of Reactor Data

Transient No.:	931
Integrated power:	205 MW-sec
Reactor period:	0.108 sec
Peak reactor power:	552 MW

Summary of Experimental Data

Fuel sample:	SPERT 1-D, 2.118 g
Sample nuclear-energy input:	676 cal/g of sample
Energy released, Al + H_2O reaction:	470 cal

Summary of Events

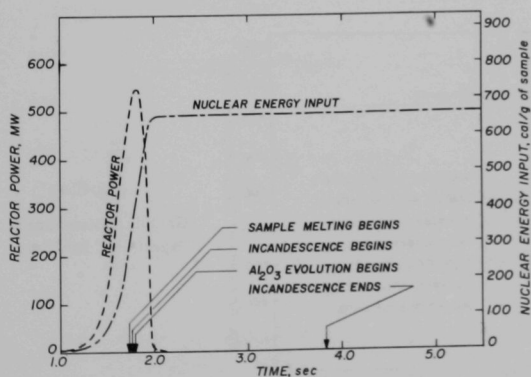|	Time, sec	Integrated Nuclear Energy, cal/g
Nucleate boiling begins	Not seen	NA
Film boiling begins	Not seen	NA
Sample melting begins	1.73	307
Incandescence begins	1.76	361
Hydrogen evolution begins	Not seen	NA
Al_2O_3 evolution begins	1.79	411
Fragmentation occurs	None	NA
Incandescence ends	3.8	NA

Fig. C.3

Graphical Summary of Experiment MWT-10

ID-103-7590

TABLE X. Tabular Summary of Experiment MWT-11

Summary of Reactor Data

Transient No.:	932
Integrated power:	220 MW-sec
Reactor period:	0.108 sec
Peak reactor power:	550 MW

Summary of Experimental Data

Fuel sample:	SPERT 1-D, 2.086 g
Sample nuclear-energy input:	726 cal/g of sample
Energy released, Al + H_2O reaction:	1190 cal

Summary of Events

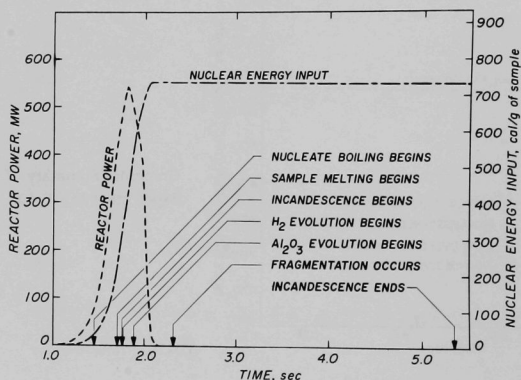|	Time, sec	Integrated Nuclear Energy, cal/g
Nucleate boiling begins	1.45	26
Film boiling begins	Not seen	NA
Sample melting begins	1.69	231
Incandescence begins	1.74	297
Hydrogen evolution begins	1.76	330
Al_2O_3 evolution begins	1.87	537
Fragmentation occurs	2.30	Transient completed at 2.05 sec
Incandescence ends	5.35	NA

Fig. C.4

Graphical Summary of Experiment MWT-11

ID-103-7591

TABLE XI. Tabular Summary of Experiment MWT-12

Summary of Reactor Data

Transient No.:	938
Integrated power:	230 MW-sec
Reactor period:	0.108 sec
Peak reactor power:	550 MW

Summary of Experimental Data

Fuel sample:	SPERT 1-D, 2.142 g
Sample nulcear-energy input:	759 cal/g of sample
Energy released, Al + H_2O reaction:	935 cal

Summary of Events

	Time, sec	Integrated Nuclear Energy, cal/g
Nucleate boiling begins	Not seen	NA
Film boiling begins	Not seen	NA
Sample melting begins	1.67	224
Incandescence begins	1.73	320
Hydrogen evolution begins	1.76	349
Al_2O_3 evolution begins	1.85	512
Fragmentation occurs	2.07	747
Incandescence ends	3.68	NA

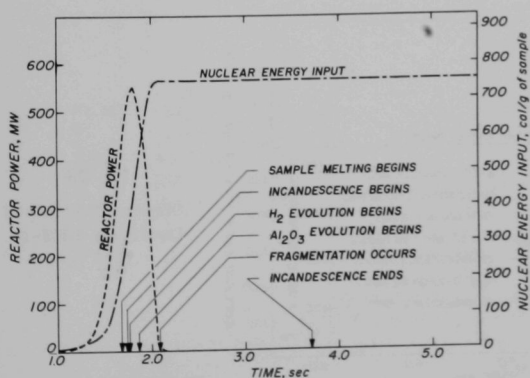
Fig. C.5

Graphical Summary of
Experiment MWT-12

ID-103-7592

TABLE XII. Tabular Summary of Experiment MWT-13

Summary of Reactor Data

Transient No.:	939
Integrated power:	176 MW-sec
Reactor period:	0.115 sec
Peak reactor power:	472 MW

Summary of Experimental Data

Fuel sample:	SPERT 1-D, 2.105 g
Sample nuclear-energy input:	582 cal/g of sample
Energy released, Al + H_2O reaction:	70 cal

Summary of Events

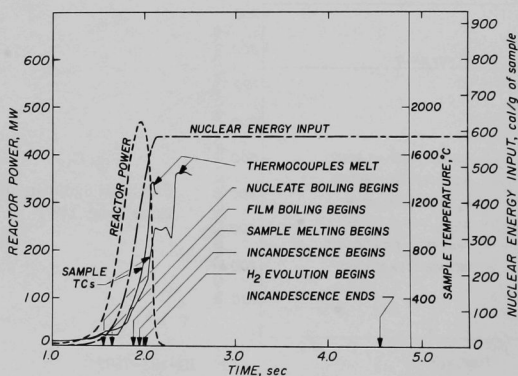|	Time, sec	Integrated Nuclear Energy, cal/g
Nucleate boiling begins	1.57	26
Film boiling begins	1.69	66
Sample melting begins	1.89	267
Incandescence begins	1.96	379
Hydrogen evolution begins	2.02	469
Al_2O_3 evolution begins	None	NA
Fragmentation occurs	None	NA
Incandescence ends	4.54	NA

Fig. C.6

Graphical Summary of Experiment MWT-13

ID-103-7593

TABLE XIII. Tabular Summary of Experiment MWT-14

Summary of Reactor Data

Transient No.:	947
Integrated power:	70 MW-sec
Reactor period:	0.285 sec
Peak reactor power:	85 MW

Summary of Experimental Data

Fuel sample:	SPERT 1-D, 2.156 g
Sample nuclear-energy input:	231 cal/g of sample
Energy released, Al + H_2O reaction:	0 cal

Summary of Events

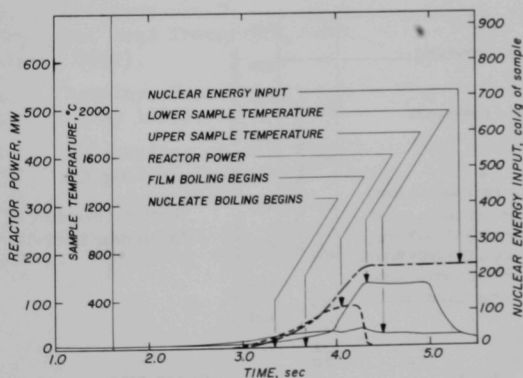|	Time, sec	Integrated Nuclear Energy, cal/g
Nucleate boiling begins	3.32	24
Film boiling begins	3.69	69
Sample melting begins	None	NA
Incandescence begins	None	NA
Hydrogen evolution begins	None	NA
Al_2O_3 evolution begins	None	NA
Fragmentation occurs	None	NA
Incandescence ends	None	NA

Fig. C.7

Graphical Summary of Experiment MWT-14

ID-103-7594

TABLE XIV. Tabular Summary of Experiment MWT-18

Summary of Reactor Data

Transient No.:	956
Integrated power:	248 MW-sec
Reactor period:	0.109 sec
Peak reactor power:	547 MW

Summary of Experimental Data

Fuel sample:	SPERT 1-D, 2.143 g
Sample nuclear-energy input:	819 cal/g of sample
Energy released, Al + H_2O reaction:	3330 cal

Summary of Events

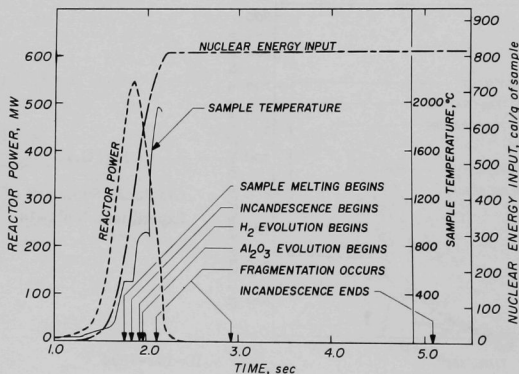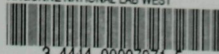|	Time, sec	Integrated Nuclear Energy, cal/g
Nucleate boiling begins	Not seen	NA
Film boiling begins	Not seen	NA
Sample melting begins	1.75	247
Incandescence begins	1.83	373
Hydrogen evolution begins	1.92	535
Al_2O_3 evolution begins	1.96	599
Fragmentation occurs	2.12 & 2.92	772 & 819
Incandescence ends	5.08	NA

Fig. C.8

Graphical Summary of Experiment MWT-18

ID-103-7595

REFERENCES

1. L. J. Harrison and R. O. Ivins, *An In-pile Photographic Study of Aluminum-clad Fuel in Water Subjected to TREAT Reactor Transients*, to be published as an ANL report.

2. M. W. Rosenthal and R. L. Miller, *An Experimental Study of Transient Boiling*, ORNL-2294 (May 1957).

3. N. A. Johnson et al., *Temperature Variation, Heat Transfer, and Void Volume Development in the Transient Atmospheric Boiling of Water*, SAN-1001 (Jan 1961).

4. Henry Lurie and N. A. Johnson, *Transient Pool Boiling of Water on a Vertical Surface with a Step in Heat Generation*, Tran. ASME J. of Heat Transfer, p. 217 (Aug 1962).

5. R. W. Miller, *An Experimental Study of Transient Boiling during SPERT-I Power Excursions*, Trans. Am. Nucl. Soc. 4, pp. 69-70 (June 1961).

6. V. R. Schrock et al., *Transient Boiling Phenomena*, SAN-1013 (May 1966).

7. T. D. Hamill and K. J. Baumeister, *Effect of Subcooling and Radiation on Film-boiling Heat Transfer from a Flat Plate*, NASA-TND-3925 (Aug 1967).

8. G. A. Fruend, P. Elias, D. R. MacFarlane, J. D. Geier, and J. F. Boland, *Design Summary Report on Transient Reactor Test Facility (TREAT)*, ANL-6034 (June 1960).

9. G. H. Golden, C. E. Dickerman, and L. E. Robinson, *Facility for Photographing In-pile Meltdown Experiments in TREAT*, ANL-6457 (Jan 1962).

10. G. L. Stephens and D. J. Campbell, *Program THTB for Analysis of General Transient Heat Transfer Systems*, General Electric No. R60FPD647 (April 1961).

11. L. A. Bromley, *Heat Transfer in Stable Film Boiling*, Chem. Eng. Prog. p. 221 (May 1950).

12. J. E. Houghtaling et al., *Transient Temperature Distribution in the SPERT-I, D-12/25 Fuel Plates during Short-period Power Excursions*, IDO-16884 (June 1964).

13. C. D. Hodgman, editor, *Handbook of Chemistry and Physics*, The Chemical Rubber Publishing Company, Cleveland (1962).